JCB Article

Poly(A)$^+$ RNAs roam the cell nucleus and pass through speckle domains in transcriptionally active and inactive cells

Chris Molenaar, Abadir Abdulle, Aarti Gena, Hans J. Tanke, and Roeland W. Dirks

Department of Molecular Cell Biology, Leiden University Medical Center, 2333 AL Leiden, Netherlands

Many of the protein factors that play a role in nuclear export of mRNAs have been identified, but still little is known about how mRNAs are transported through the cell nucleus and which nuclear compartments are involved in mRNA transport. Using fluorescent 2′*O*-methyl oligoribonucleotide probes, we investigated the mobility of poly(A)$^+$ RNA in the nucleoplasm and in nuclear speckles of U2OS cells. Quantitative analysis of diffusion using photobleaching techniques revealed that the majority of poly(A)$^+$ RNA move throughout the nucleus, including in and out of speckles (also called SC-35 domains), which are enriched for splicing factors. Interestingly, in the presence of the transcription inhibitor 5,6-dichloro-1-β-D-ribofuranosylbenzimidazole, the association of poly(A)$^+$ RNA with speckles remained dynamic. Our results show that RNA movement is energy dependent and that the proportion of nuclear poly(A)$^+$ RNA that resides in speckles is a dynamic population that transiently interacts with speckles independent of the transcriptional status of the cell. Rather than the poly(A)$^+$ RNA within speckles serving a stable structural role, our findings support the suggestion of a more active role of these regions in nuclear RNA metabolism and/or transport.

Introduction

Gene expression is a multistep process that involves transcription, RNA processing, nuclear RNA export, cytoplasmic RNA transport, and translation. Nuclear RNA export has recently been recognized as being an important potential mechanism to regulate gene expression, but has not yet been completely characterized. As a result of gene expression, different classes of RNA, including rRNA, mRNA, snRNA, and tRNA, are produced and transported to the cytoplasm via distinct transport pathways (Jarmolowski et al., 1994; Cullen, 2003). In the case of mRNA, there is evidence that mRNA transport is tightly coupled to mRNA synthesis and processing. Recruitment of nuclear mRNA export factors to transcripts has been coupled to different steps in gene expression including transcription (Lei et al., 2001; Strasser et al., 2002), splicing (Luo and Reed, 1999; Zhou et al., 2000; Le Hir et al., 2001; Luo et al., 2001), and 3′ end formation (Lei and Silver, 2002). Furthermore, the presence of unstructured regions in mRNAs has recently been implicated as mediating recognition by export factors (Ohno et al., 2002). A tight coupling between splicing and nuclear mRNA export would explain why only spliced RNAs are transported to the cytoplasm. The exon junction complex is a protein complex that contains, among other proteins, the mRNA export factor REF1/Aly. It assembles upstream of splice junctions upon pre-mRNA splicing and has been proposed to mediate this coupling through interaction of REF1/Aly with the major receptor for mRNA export, TAP (Le Hir et al., 2001). However, recent works indicate that the exon junction complex proteins may contribute to nuclear mRNA export but are not essential (Gatfield and Izaurralde, 2002). Instead, SR splicing factors that bind to mRNA were shown to interact directly with TAP for efficient export (Huang et al., 2003).

Splicing factors are also considered to be indispensable for retaining pre-mRNAs in the cell nucleus. Pre-mRNAs were shown to accumulate at or near active sites of transcription and to colocalize with splicing factors (Bauren et al., 1996; Dirks et al., 1997; Misteli et al., 1997). Also, transcripts defective in splicing were shown to accumulate at sites of

Address correspondence to R.W. Dirks, Dept. of Molecular Cell Biology, Leiden University Medical Center, Wassenaarseweg 72, 2333 AL Leiden, Netherlands. Tel.: 31-71-5276026. Fax.: 31-71-5276180. email: r.w.dirks@lumc.nl

Key words: RNA transport; mRNA; 2′*O*-methyl RNA; FRAP; live cell imaging

Abbreviations list: DRB, 5,6-dichloro-1-β-D-ribofuranosylbenzimidazole; FLIP, fluorescence loss in photobleaching; HCMV, human cytomegalovirus; PABP2, poly(A) binding protein II; TAMRA, tetramethylrhodamine.

The Journal of Cell Biology, Volume 165, Number 2, April 26, 2004 191–202
http://www.jcb.org/cgi/doi/10.1083/jcb.200310139

The Journal of Cell Biology

transcription and unable to be exported to the cytoplasm (Custodio et al., 1999). Therefore, it is assumed that most mRNAs are released from their site of synthesis and processing after completion of splicing. These mRNAs move randomly within the cell nucleus with export factors associated with them before they get bound to a nuclear pore complex and enter the cytoplasm. This assumption is supported by fluorescence in situ hybridization and BrUTP labeling studies showing that specific gene transcripts emanate from transcription sites in all directions in cell nuclei (Zachar et al., 1993; Dirks et al., 1995; Macville et al., 1995; Singh et al., 1999). Furthermore, in vivo hybridization studies revealed that poly(A)$^+$ RNA moves randomly in the cell nucleus at a rate compatible with free diffusion (Politz et al., 1998, 1999).

However, various aspects of nuclear RNA export are unclear. These aspects include the role of nuclear compartments in the export process. Speckles, also referred to as SC-35 domains, are nuclear compartments that contain a large number of factors required for mRNA synthesis, processing, and export (Lamond and Spector, 2003). The observation that speckles also contain poly(A)$^+$ RNA led to the suggestion that speckles themselves may play a role in RNA metabolism and export (Carter et al., 1991, 1993). These speculations were supported by the observation that sites of bromouridine incorporation that mark nascent transcripts overlap with speckles (Wei et al., 1999) and that some specific active genes localize at the edges of speckles (Xing et al., 1993, 1995; Smith et al., 1999; Shopland et al., 2003). Furthermore, a number of specific gene transcripts were shown to localize to the inside of speckles (Puvion and Puvion-Dutilleul, 1996; Smith et al., 1999; Johnson et al., 2000; Melcak et al., 2000; Hattinger et al., 2002; Shopland et al., 2002, 2003), indicating that speckles play a direct role in mRNA metabolism and export. However, various lines of evidence argue against a direct role of speckles in gene transcription, RNA processing, and RNA transport. First, in contrast to Wei et al. (1999), several reports indicate that speckles are not labeled after ^{3}H- or bromouridine incorporation (Fakan, 1994; Cmarko et al., 1999). Second, splicing factors were shown to be recruited from speckles to sites of active transcription (Jimenez-Garcia and Spector, 1993; Huang and Spector, 1996; Dirks et al., 1997; Misteli et al., 1997; Zeng et al., 1997; Snaar et al., 1999). Third, poly(A)$^+$ RNA is not exported from speckles when transcription is inhibited and is, therefore, suggested to be a stable population that plays a structural role and acts as a binding site for RNA processing proteins (Huang et al., 1994; Sacco-Bubulya and Spector, 2002). Finally, in vivo hybridization experiments using oligo (dT) probes that hybridize to the poly(A) tails of mRNAs in living cells did not reveal any accumulation of poly(A)$^+$ RNA in speckles at any stage of transport (Politz et al., 1999).

To investigate a possible role for speckles in RNA transport, we analyzed the mobility of poly(A)$^+$ RNA in the nucleoplasm and in nuclear speckles in transcriptionally active and inactive cells. Using 2'*O*-methyl RNA probes and photobleaching techniques, we demonstrate that poly(A)$^+$ RNA moves throughout the nucleoplasm, though at a much slower rate compared with transport rates determined in previous works using oligodeoxynucleotide probes and compared with proteins that play a role in RNA processing and transport. Furthermore, we present evidence that poly(A)$^+$ RNA transiently interacts with speckle domains independent of transcription but dependent on cellular energy levels.

Results

The poly(A)$^+$ RNA fractions in nucleoplasm and speckles reveal similar kinetic behavior

Poly(A)$^+$ RNA was visualized in nuclei of living U2OS cells by means of a tetramethylrhodamine (TAMRA)-labeled 2'OMe $(U)_{22}$ probe that is complementary to the poly(A) tail of mRNAs. Shortly after injection into the cytoplasm of U2OS cells, this probe revealed a nuclear localization pattern that is characteristic for poly(A)$^+$ RNA (Carter et al., 1991). In addition to a diffuse staining of the nucleoplasm, excluding nucleoli, a speckled staining was observed. The cytoplasm of cells revealed only a very weak fluorescence staining. The movement of poly(A)$^+$ RNA in the cell nucleus was studied using FRAP and fluorescence loss in photobleaching (FLIP) analysis. For this purpose, we selected cells with moderate levels of fluorescence signals. Images of a typical FRAP experiment are shown in Fig. 1. In the top cell in Fig. 1 A, a speckle was bleached (green circle), and the cell was subsequently imaged as described in Materials and methods. Using a bleaching pulse of 5 s, it was possible to bleach the area down to only ~20% of the initial intensity. The recovery of poly(A)$^+$ RNA fluorescence in the speckle, as a consequence of movement of unbleached poly(A)$^+$ RNA from the surroundings into the bleached area, is clearly visible in the pseudo-color images (Fig. 1 A). Next, we determined the average $t_{1/2}$ of recovery and the diffusion coefficient (D) for poly(A)$^+$ RNA in speckles from the derived FRAP curves (Fig. 1 C): $t_{1/2} \approx 26$ s, D ≈ 0.03 $\mu m^2/s$ (Table I). During the time course of the experiment, the fluorescence in the speckles did not recover completely, suggesting that a relatively immobile fraction of poly(A)$^+$ RNA of ~15% exists in these compartments.

To confirm that, we photobleached 2'OMe $(U)_{22}$-TAMRA that localized to speckles, we also injected the probe in U2OS cells that express SF2/ASF-GFP. In these cells, speckles, identified by the presence of SF2/ASF-GFP, were selected for photobleaching the TAMRA-labeled probe. The recovery times measured for the 2'OMe $(U)_{22}$ probe in SF2/ASF-GFP–labeled speckles were similar to the ones measured in the nontransfected cells (unpublished data).

Next, we photobleached nucleoplasmic areas at some distance from a speckle and analyzed the recovery of fluorescence. The recovery appeared to be ~1.5 times faster (Fig. 1, B and D): $t_{1/2} \approx 18$ s, D ≈ 0.04 $\mu m^2/s$ (Table I). These experiments suggest a difference in mobility between the poly(A)$^+$ RNA fractions inside the speckles and poly(A)$^+$ RNA fractions outside the speckles. However, in cells where only a part of a speckle was bleached, the calculated diffusion constants appeared to be in the order of 0.035 $\mu m^2/s$. The discrepancy in estimated D-values could result from the difference in the number of molecules present in the bleached area relative to those in the vicinity of the bleached area.

It is likely that the majority of the poly(A)$^+$ RNA that moves into the bleached area initially comes from the immediate vicinity of the bleached spot. To determine the freedom of movement of poly(A)$^+$ RNA throughout the nucleoplasm,

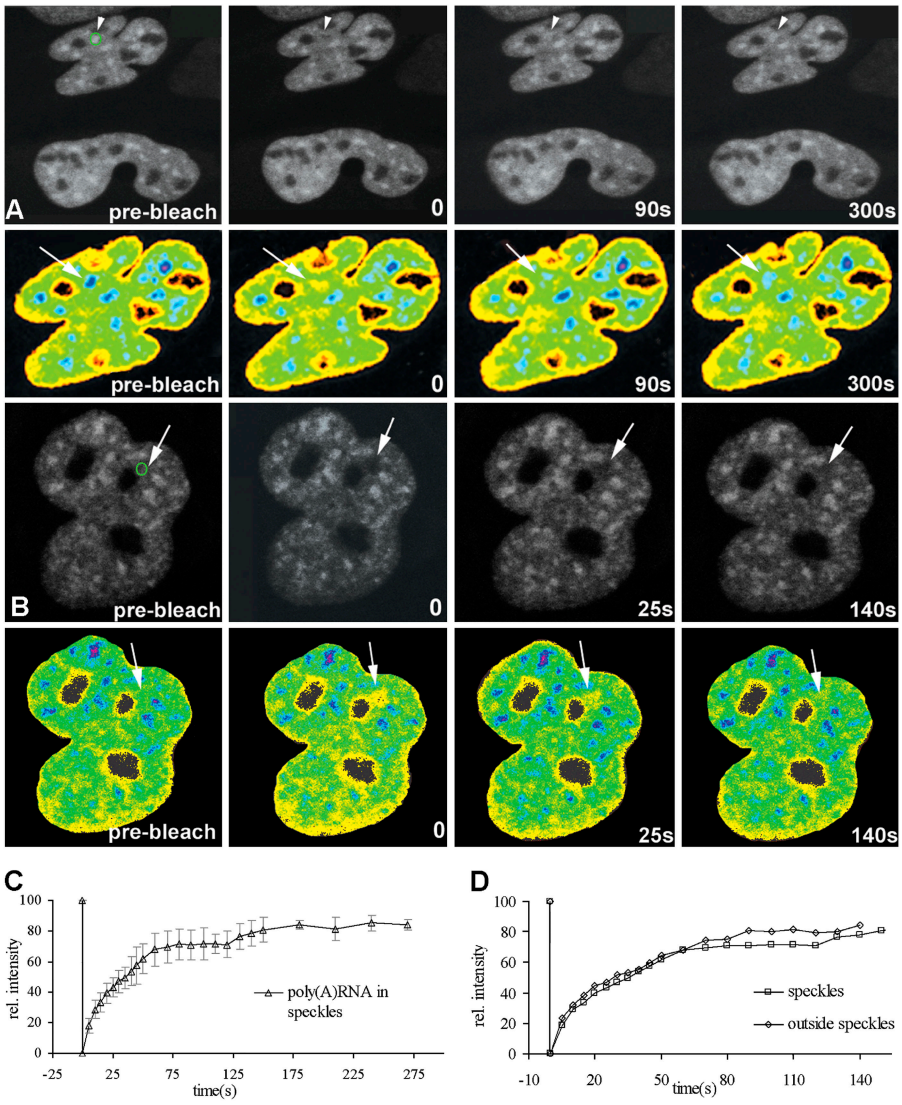

Figure 1. **FRAP analysis of fluorescent 2′OMe $(U)_{22}$ demonstrates that poly(A)$^+$ RNA is a dynamic component of speckles and nucleoplasm.** Living U2OS cells injected with $(U)_{22}$-TAMRA were subjected to FRAP analysis. A speckle (A) and a nucleoplasmic area outside a speckle (B) were selected and photobleached. Images were recorded just before bleaching and at different time intervals after bleaching. The green circles indicate the photobleached region. To illustrate the recovery of fluorescence more clearly, pseudocolor images of the bleached cells are shown. Fluorescence intensities range from yellow (low) to blue (high). The fluorescence recovery in the bleached areas, indicated by arrows and arrowheads, was quantified, and relative fluorescence intensities, which were calculated as described in Materials and methods, are displayed in recovery curves (C and D). The measurement immediately after bleaching was set at 0 s. In speckles, fluorescence recovery reached a plateau at ~85% around 250 s (C). The error bars represent SD. (D) The recovery curve from a bleached area outside a speckle is compared with one obtained from a bleached speckle. The curves shown in C and D represent the average values of 15 measured cells.

including speckles, we applied FLIP. A spot in the nucleoplasm was repeatedly bleached for 3 s with 10-s time intervals in which images of the cell were recorded. Fig. 2 shows the result of a typical FLIP experiment. Loss of total nuclear fluorescence was imaged (Fig. 2 A) and measured over time (Fig. 2 B). After 400 s from the first bleach, ~85% of the nuclear poly(A)$^+$ RNA fluorescence was lost. Similar results were obtained when a region inside a speckle was repeatedly photobleached, suggesting that the mobility of poly(A)$^+$ RNA in the nucleoplasm and speckles is very similar. The fraction of ~15% of the total amount of fluorescence that is still present in the nucleus after 400 s bleaching suggests the presence of a relatively immobile population of poly(A)$^+$ RNA, which is in agreement with the result of the FRAP experiments.

To determine if the FLIP curve represents a single population of moving poly(A)$^+$ RNA, the curve was converted to a semi-logarithmic plot and analyzed by curve fitting. The result revealed a single exponential fit, suggesting the existence of a "single" population of moving poly(A)$^+$ RNA (Fig. 2 C). Hence, the fraction of poly(A)$^+$ RNA or unbound probe that diffuses rapidly through the nucleus appears to be very small, if present at all. To confirm this finding, we also measured the fluorescence intensity of regions outside a photobleached spot immediately before and after photobleaching in 10 cells. By comparing the intensities and compensating for photobleaching (using another cell in the same microscopic field as a reference), we measured reductions in intensity between 3–5%, suggesting that there may exist a small free diffusing pool of probe and/or poly(A)$^+$ RNA (unpublished data).

No significant loss of signal was observed when the bleached spot was set in nucleoli or cytoplasm (unpublished data). These results imply that most poly(A)$^+$ RNA is moving throughout the nucleoplasm, except for nucleoli. However, we cannot exclude that low amounts of poly(A)$^+$ RNA move through nucleoli. Prolonged periods of photobleaching a spot in a nucleolus resulted in some loss of fluorescent signal in the nucleoplasm, which could be due to the photobleaching of fluorescent probe either present in nucleoli or in the nucleoplasm above or below nucleoli.

2′OMe $(U)_{22}$ localization and kinetics are dependent on the presence of poly(A) tails

To confirm that 2′OMe $(U)_{22}$ probe molecules hybridize specifically to the poly(A) tail of RNAs, cells were treated

Table I. **Diffusion times and coefficients measured for the different probes used in this paper**

	$t_{1/2}$ recovery	D
	s	$\mu m^2/s$
Poly(A)$^+$ RNA (37°C)		
speckles	26	0.03
nucleoplasm	18	0.04
U1 snRNA	4.5	0.16
HCMV-IE mRNA	0.3	1.9
d(T)$_{40}$-probe	0.35	1.7

Values for $t_{1/2}$ and D were determined as described in Materials and methods.

with cordycepin, which prevents poly(A) addition but does not block RNA synthesis (Darnell et al., 1971; Mendecki et al., 1972; Calado and Carmo-Fonseca, 2000). It was predicted that after cordycepin treatment the 2'OMe $(U)_{22}$ probe would not localize to poly(A)$^+$ rich speckle domains and would reveal a fast movement consistent with free diffusion. U2OS cells were incubated with cordycepin for 16 h, injected with 2'OMe $(U)_{22}$ probe, and imaged by confocal microscopy. Consistent with our prediction, the 2'OMe $(U)_{22}$ probe revealed a diffuse staining in the nucleus excluding nucleoli (Fig. 3, A and B). Also, as determined by FRAP (Fig. 3, A and C) and FLIP (Fig. 3, B and D), the mobility of the 2'OMe $(U)_{22}$ probe was significantly increased in cordycepin-treated cells compared with nontreated cells. These findings demonstrate that the 2'OMe $(U)_{22}$ probe binds with high specificity to the poly(A) tail of RNAs. Furthermore, the results show that the preferential association of the 2'OMe $(U)_{22}$ probe with speckles results from their interaction with poly(A)$^+$ RNA in living cells. This result is consistent with our finding that the 2'OMe $(U)_{22}$ probe is highly specific for poly(A)$^+$ RNA in fixed cells as determined by RNase controls (Molenaar et al., 2001).

Oligodeoxynucleotide $(dT)_{40}$ moves significantly faster through the nucleoplasm compared with 2'OMe $(U)_{22}$

The estimated diffusion coefficient for poly(A)$^+$ RNA movement in this work is significantly lower than determined in previous works (Politz et al., 1998, 1999). To explain this discrepancy, we compared the localization and the dynamic behavior of the 2'OMe $(U)_{22}$ probe with that of a poly(A) tail-specific oligodeoxynucleotide $(dT)_{40}$ probe, a probe type that has been used in previous papers, a complementary 2'OMe $(A)_{18}$ negative control probe, and a 2'OMe human cytomegalovirus (HCMV) negative control probe (specific for cytomegalovirus immediate-early mRNA) in living U2OS cells. The $(dT)_{40}$ probe revealed a diffuse staining of the nucleoplasm and a moderate staining of nucleoli and, significantly, revealed no accumulation in speckles (Fig. 4 A). Furthermore, FRAP analysis of the oligo $(dT)_{40}$ probe revealed a $t_{1/2}$ of recovery of 0.35 s and a diffusion coefficient of $\sim$1.7 $\mu m^2/s$ (Fig. 4, A and B; and Table I). Hence, the oligo $(dT)_{40}$ probe appears to move $\sim$50-fold faster than the 2'OMe $(U)_{22}$ probe, suggesting that only a small proportion of microinjected oligo $(dT)_{40}$ probe binds to poly(A)$^+$ RNA and that the majority of the probe moves by free diffusion

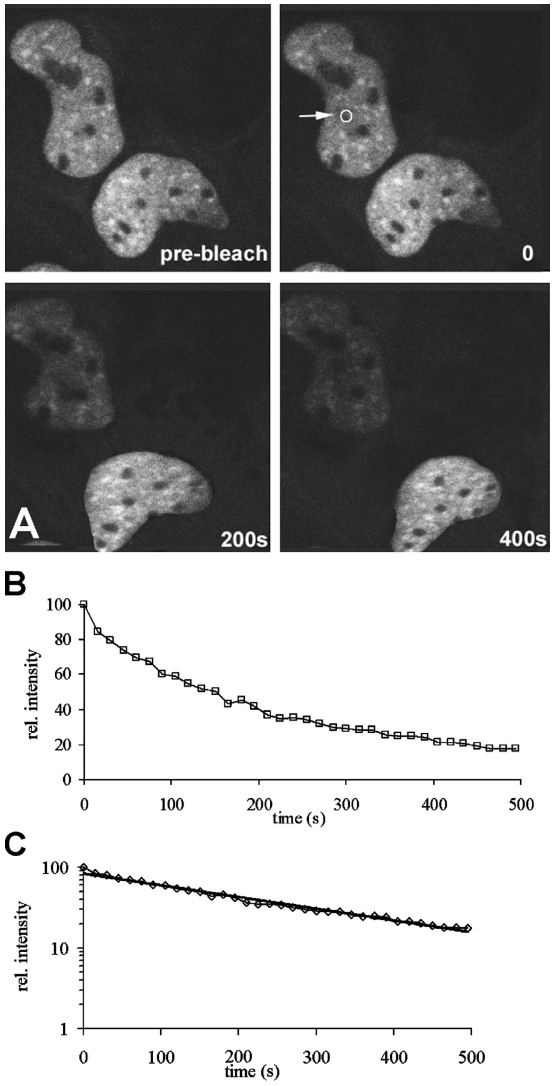

Figure 2. **FLIP analysis of fluorescent 2'OMe $(U)_{22}$ shows that poly(A)$^+$ RNA moves throughout the nucleus.** (A) The fluorescence intensity of the top cell gradually decreases when a spot (arrow) is repeatedly bleached. (B) The corresponding FLIP curve shows that a relative immobile fraction of $\sim$15% remains present. (C) Semi-logarithmic plot of nuclear loss of fluorescence shows that the curve can be fitted to a single exponential fit, indicating a single population of slow moving poly(A)$^+$ RNA.

through the nucleoplasm. Also, the probes 2'OMe $(A)_{18}$ and 2'OMe HCMV revealed a diffuse nuclear staining and rapid movement in U2OS cells. Like the 2'OMe $(A)_{18}$-TAMRA probe (not depicted), 2'OMe HCMV-TAMRA could not be photobleached in defined areas to $<$80% of the initial intensity (Fig. 4 C), indicating a high rate of diffusion. The corresponding FRAP curves confirm the fast movement of 2'OMe HCMV probe compared with 2'OMe $(U)_{22}$ in cell nuclei by showing a rapid recovery of fluorescence to $\sim$100% after bleaching (Fig. 4 D). For 2'OMe HCMV, a $t_{1/2}$ recovery time of 0.3 s and a diffusion constant of 1.9 $\mu m^2/s$ was calculated, which is $\sim$60-fold higher than measured for the 2'OMe $(U)_{22}$ probe (Table I). To confirm these FRAP results, we analyzed the kinetic behavior of the control probes by FLIP. As shown in Fig. 4 (E–H), the control probes re-

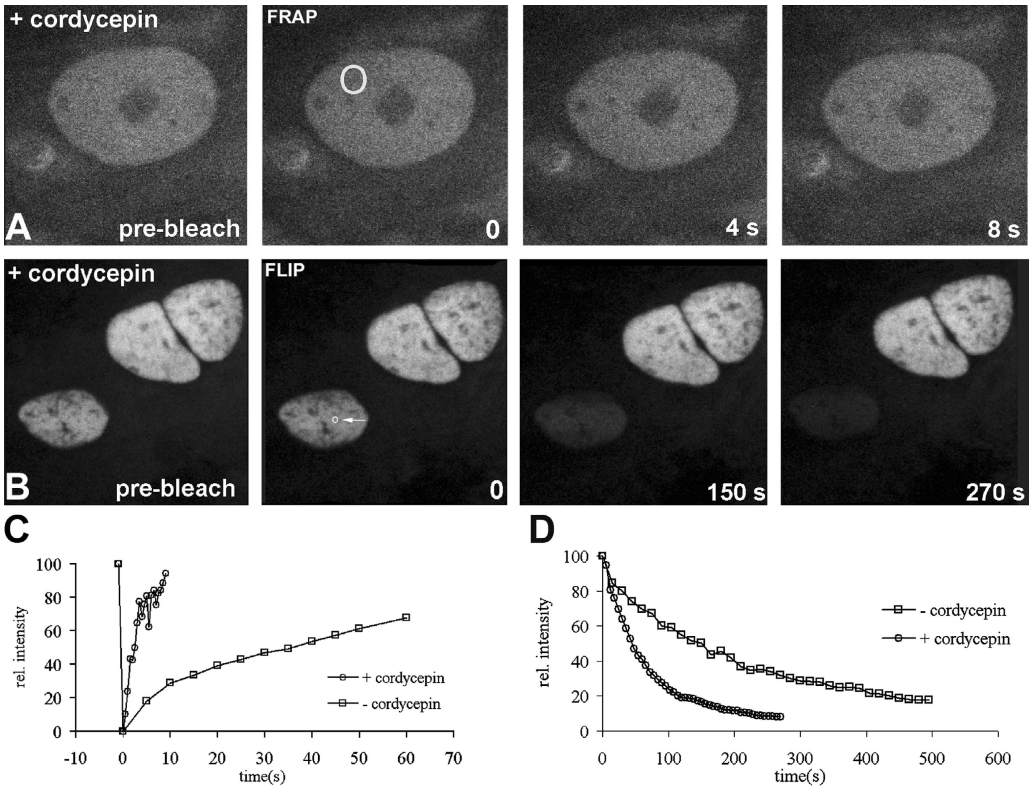

Figure 3. **Diffuse nuclear staining and high mobility rate of 2′OMe $(U)_{22}$ in cordycepin-treated cells.** The localization pattern of 2′OMe $(U)_{22}$ in cordycepin-treated cells reveals that the probe is diffusely spread throughout the nucleoplasm and not concentrated in speckles. Both FRAP (A and C) and FLIP (B and D) analysis revealed a mobility rate that is significantly higher compared with untreated cells, indicating that the mobility rate is strongly dependent on specific hybridization to poly(A)$^+$ RNA. The circles indicate the bleached areas.

vealed much faster kinetic behavior than 2′OMe $(U)_{22}$. Together with the cordycepin experiment, these results strongly indicate that the 2′OMe $(U)_{22}$ probe hybridizes stably and specifically to poly(A)$^+$ RNA in living U2OS cells.

To compare the kinetics of 2′OMe $(U)_{22}$ movement with that of another probe that is supposed to hybridize to a target sequence in speckles, we designed a 2′OMe RNA probe specific for U1snRNA. U1snRNA is a component of the U1snRNP complex that is involved in RNA splicing and is present throughout the nucleoplasm and in Cajal bodies and, like poly(A)$^+$ RNA, is concentrated in nuclear speckles (Lamond and Carmo-Fonseca, 1993). After injection of the 2′OMe RNA probe specific for U1snRNA in U2OS cells, we observed fluorescence signals emerging in these structures, indicating that this probe specifically hybridized to U1snRNA (Fig. 5 A). Subsequent FRAP analysis revealed that the 2′OMe U1snRNA-specific probe has a 4–5-fold higher rate of movement (Table I, $t_{1/2} \approx 4.5$ s, D $\approx$ 0.16 $\mu m^2/s$) than poly(A)$^+$ RNA in speckles (Fig. 5 B). Nevertheless, the rate of 2′OMe U1snRNA movement is considerably slower than measured for the probes 2′OMe $(A)_{18}$ and 2′OMe HCMV.

Poly(A)$^+$ RNAs enter and leave speckles in 5,6-dichloro-1-β-D-ribofuranosylbenzimidazole (DRB)–treated cells

Inhibition of RNA polymerase II transcription by DRB (Sehgal et al., 1976) was shown to result in a redistribution of poly(A)$^+$ RNA in cell nuclei characterized by the disappearance of a nucleoplasmic pool and the maintenance of a stable population of poly(A)$^+$ RNA concentrated in speckles along with pre-mRNA splicing factors (Huang et al., 1994). To investigate the influence of RNA polymerase II transcription inhibition on the mobility of poly(A)$^+$ RNA, we analyzed the dynamic properties of hybridized 2′OMe $(U)_{22}$ probe in DRB-treated cells by FLIP. Cells were analyzed after treatment with DRB for 4 h either before or after microinjection of the 2′OMe $(U)_{22}$ probe. As expected, a typical enlargement and rounding-up of the speckles was observed (Fig. 6 A). To measure the mobility of the hybridized 2′OMe $(U)_{22}$ probe in speckles, a speckle was selected and continuously photobleached using a high-intensity laser beam. Fig. 6 B illustrates the loss of nuclear fluorescence due to continuous photobleaching of a speckle in a DRB-treated cell. The corresponding FLIP curves show a gradual loss of fluorescence in all speckles of DRB-treated cells at a rate that is similar to the one observed for nontreated cells (Fig. 6 C), indicating that nearly all poly(A)$^+$ RNAs present in speckles are mobile and leave speckles independently of the transcriptional activity of the cell.

The uptake of poly(A)$^+$ RNA by speckles is energy dependent

To investigate whether or not the movement of poly(A) RNA toward speckles requires energy, we performed photobleaching experiments using cells maintained at 22 and 37°C. When compared, the typical localization pattern of

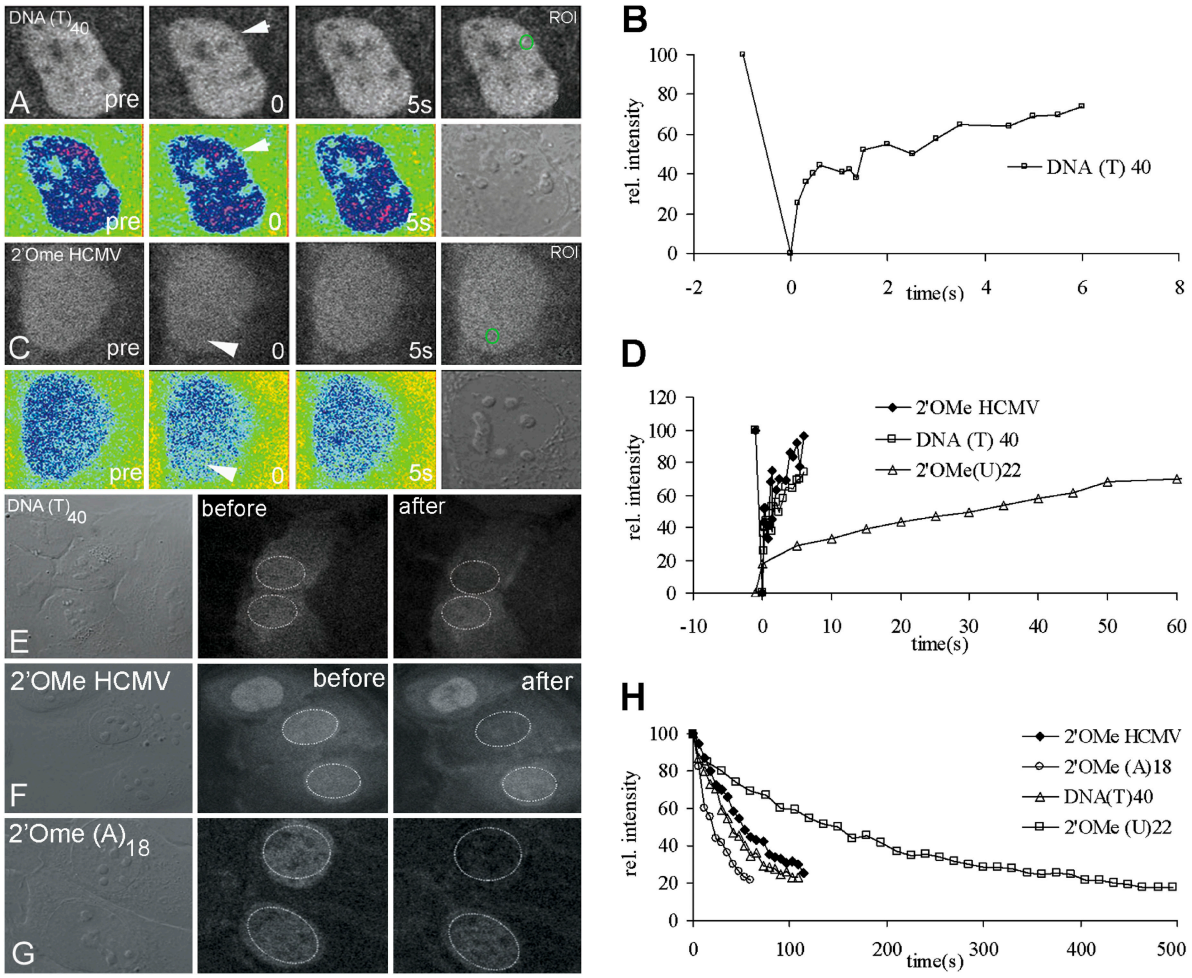

Figure 4. **FRAP and FLIP analysis show that control probes are highly mobile.** (A) In U2OS cells, the TAMRA-labeled $(dT)_{40}$ probe reveals a diffuse staining of the nucleoplasm, excluding nucleoli, after cytoplasmic microinjection. Bleaching of a selected area (green circle and arrows) resulted in a rapid recovery of fluorescence. Due to the rapid movement of the probe, the fluorescence intensity immediately after bleaching had already returned to ~80% of the initial fluorescence, whereas within a few seconds a recovery to ~100% was observed. Quantitative analysis of the FRAP measurements confirms the high mobility of the $(dT)_{40}$ probe (B) and shows that $(dT)_{40}$ moves much faster through the nucleus compared with the 2′OMe $(U)_{22}$ probe (D). Similar kinetics were observed using the control probe 2′OMe HCMV that has no target in U2OS cells (C and D). (C) The circle and arrowheads indicate the bleached areas. Fluorescence intensities are also represented in pseudocolor, and the differential interference contrast images are recorded after the bleaching experiment showing that the bleached cells are not affected by the experimental conditions. FLIP analysis of cells injected with $(dT)_{40}$ (E), 2′OMe HCMV (F), and 2′OMe $(A)_{18}$ (G) reveals that these probes move significantly faster through the nucleoplasm than the 2′OMe $(U)_{22}$ probe (H).

poly(A)$^+$ RNA was unaltered by the temperature change. In cells maintained at 22°C, speckles were selected and photobleached, and the recovery of fluorescence in the defined areas was imaged and measured. A typical example of this process is shown in Fig. 7 A. A speckle indicated in the prebleach image was photobleached, and the fluorescence recovery is shown at 0, 90, and 270 s after bleaching. Fluorescence did not fully recover in the bleached speckle. Fluorescence recovery values were also measured, and the corresponding recovery curves, each collected from 15 cells, show a slower recovery of fluorescence in speckles at 22°C compared with 37°C (Fig. 7 B). Significantly, not more than 50% fluorescence recovery was measured at 22°C. Similar fluorescence recovery results were obtained from nucleoplasmic areas at some distance from speckles that were photobleached and imaged at increasing time intervals (unpublished data). Together, these results suggest that poly(A)$^+$ RNA transport through the nucleoplasm and into speckles requires energy.

RNA-associating proteins show different kinetic behaviors than poly(A)$^+$ RNA

Next, we investigated how the dynamic behavior of proteins that directly or indirectly associate with mRNA correlates with poly(A)$^+$ RNA dynamics. We analyzed the mobility of the splicing protein SF2/ASF, of the poly(A) tail binding protein PABP2 (poly(A) binding protein II), and of the transport proteins Aly and Tap, all tagged with GFP, in living U2OS cells using FRAP. Previously, these GFP fusion proteins were shown to localize and to function similarly to their endogenous counterparts (Misteli et al., 1997; Katahira et al., 1999; Zhou et al., 2000; Calapez et al., 2002).

To measure the mobility of SF2/ASF-GFP relative to the mobility of poly(A)$^+$ RNA, we microinjected U2OS cells

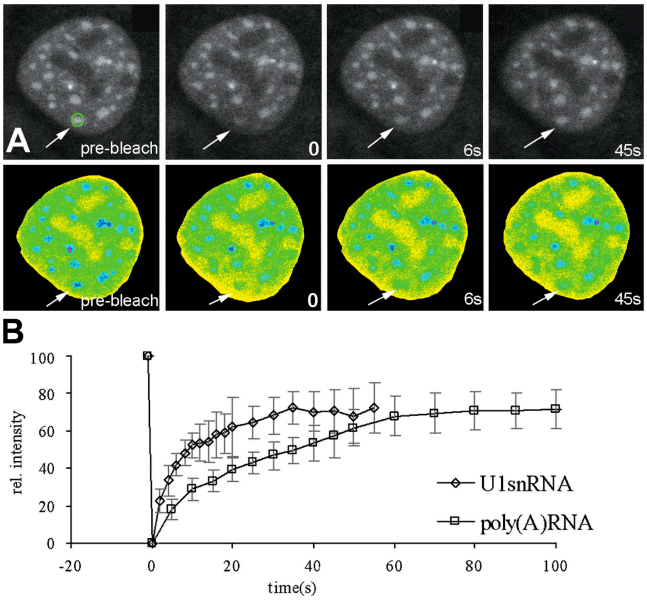

Figure 5. **2′OMe U1snRNA-TAMRA localizes to speckles and has a higher mobility rate than 2′OMe (U)$_{22}$.** After cytoplasmic microinjection, 2′OMe U1 snRNA-TAMRA localizes to nucleoplasm, speckles, and Cajal bodies (two bright dots), but not to nucleoli. The mobility of this probe was analyzed by FRAP. Images were recorded just before, immediately after, and at regular time intervals after photobleaching. (A) 4 images out of a series of 26 are displayed, and the arrow indicates the speckle that has been photobleached. (B) The corresponding FRAP curve is plotted together with the FRAP curve for 2′OMe (U)$_{22}$-TAMRA, indicating that U1snRNA is more dynamic than poly(A)$^+$ RNA in cell nuclei. The error bars represent SD.

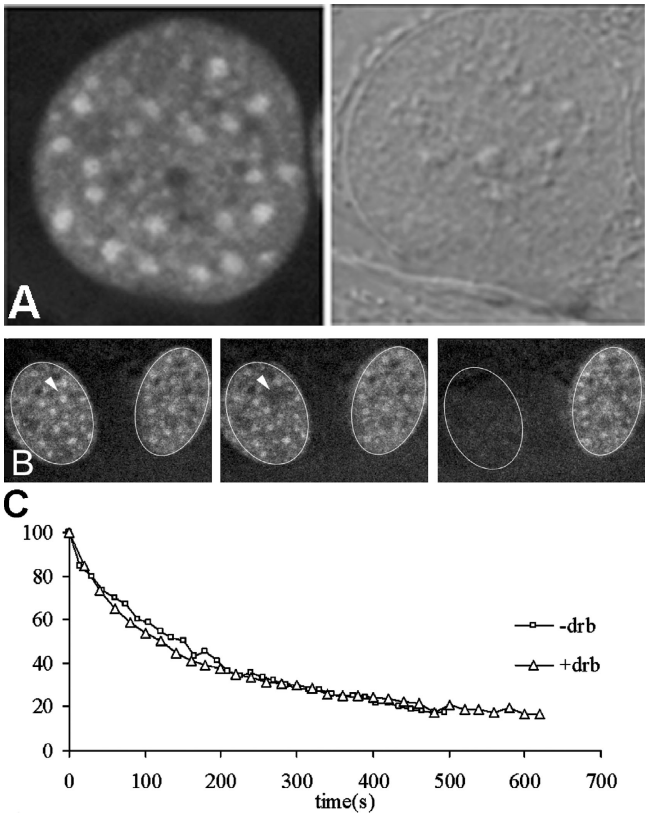

Figure 6. **DRB treatment does not reduce the mobility of poly(A)$^+$ RNA.** After microinjection of the 2′OMe (U)$_{22}$-TAMRA probe, DRB was added to the medium to a final concentration of 50 μg/ml, and FLIP analysis was performed 3–4 h later. Incubation with DRB resulted in enlargement and rounding-up of speckles (A), whereas the morphology of the cell nucleus was not affected as shown in the differential interference contrast image. FLIP analysis of DRB-treated cells revealed no significant difference in the rate of fluorescence loss between treated and nontreated cells (B and C). The arrowhead is indicating the speckle that has been repeatedly bleached at high laser power.

stably expressing SF2/ASF-GFP with the 2′OMe (U)$_{22}$-TAMRA probe and analyzed them by FRAP. SF2/ASF-GFP and the probe 2′OMe (U)$_{22}$-TAMRA were photobleached simultaneously in a speckle, and the fluorescence recovery of both fluorophores was imaged separately at each time point in a time series to prevent cross talk. Fig. 8 A illustrates that the fluorescence recovery of SF2/ASF-GFP in a photobleached speckle precedes that of poly(A)$^+$ RNA. Hence, SF2/ASF-GFP seems significantly more mobile than poly(A)$^+$RNA. This difference in fluorescence recovery was confirmed by comparing the calculated FRAP curves obtained from eight cells (Fig. 8 D).

It was shown previously that the localization of PABP2 in speckles is dependent on binding to poly(A)$^+$ RNA (Calado et al., 2000). Therefore, we were interested to compare the mobility of transiently expressed PABP2-GFP toward speckles with that of poly(A)$^+$ RNA by FRAP in U2OS cells. For this purpose, PABP2-GFP–containing speckles were photobleached and the fluorescence recovery rates were subsequently imaged. The results show that a nearly complete fluorescence recovery is obtained within 50 s (Fig. 8 B) and suggest that SF2/ASF-GFP and PABP-GFP move in and out of speckles faster than poly(A)$^+$ RNA (Fig. 8 D).

Because Aly and Tap have been implicated in playing roles in mRNA export and Aly has been shown to accumulate in nuclear speckles, we expected that the kinetics of Aly and Tap movement would correlate with the kinetic behavior of poly(A)$^+$ movement. Fig. 8 C shows the localization pattern of Aly-GFP as observed in U2OS cells and a speckle that has been photobleached and subsequently imaged at regular time intervals afterwards. As shown, a full recovery of fluorescence is obtained within 1 min after photobleaching (Fig. 8 C). Also, the FRAP curve that has been generated after measuring recovery values in speckles from 10 cells shows that a near full recovery is obtained within 1 min (Fig. 8 E).

Next, we determined the dissociation kinetics of Aly-GFP from speckles by FLIP. Repeated bleaching of Aly-GFP in a defined area using high laser power revealed that the majority of Aly-GFP fluorescence was lost from the nucleus within 80 s (Fig. 8 F). When we performed similar experiments with cells expressing the RNA export factor Tap-GFP and its cofactor p15, which distributes more or less homogeneously throughout the nucleoplasm, we observed a loss of nuclear fluorescence within 60 s (Fig. 8 F). These results show that the transport factors Tap and Aly move more rapidly through the cell nucleus compared with the 2′OMe (U)$_{22}$ probe hybridized to poly(A)$^+$ RNA (Fig. 2) and suggest that there is a significant fraction of unbound Tap and Aly present in cell nuclei.

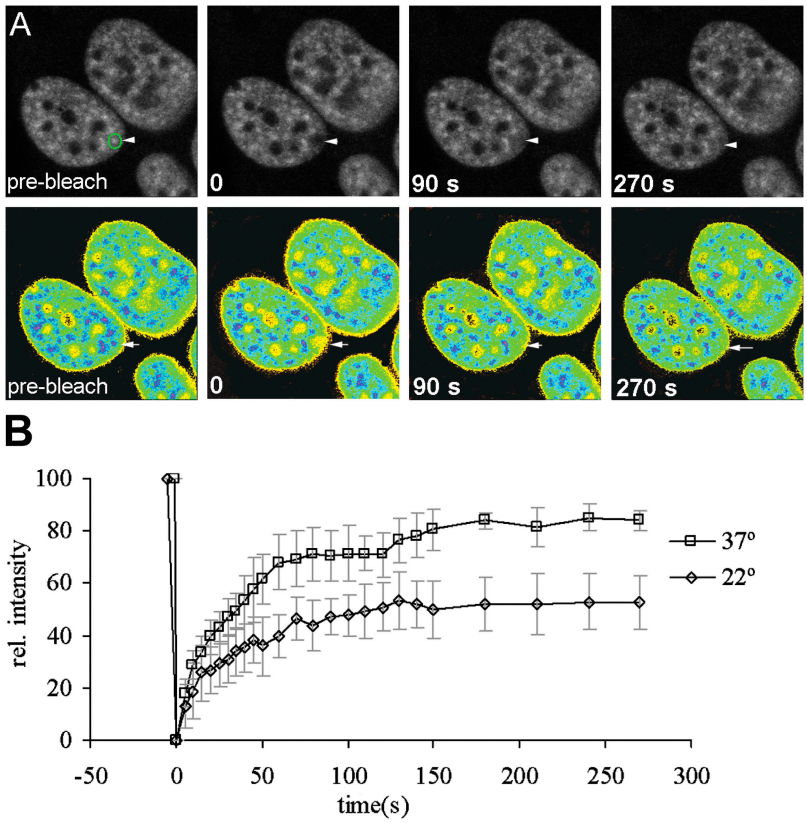

Figure 7. **The import of poly(A)$^+$ RNA into speckles is reduced at 22°C.** Cells microinjected with 2′OMe $(U)_{22}$-TAMRA were incubated at either 37or 22°C and subjected to FRAP analysis. At each temperature, 15 cells were analyzed. (A) Confocal images out of a series of 26 show the recovery of fluorescence within a speckle (green circle) at different time points after photobleaching (arrowheads and arrows) in cells kept at 22°C. (B) The recovery curves of cells incubated at 37 or 22°C are plotted with error bars representing SD.

Discussion

Using 2′OMe RNA probes, we analyzed the kinetics of poly(A)$^+$ RNA localization in living U2OS cells. Poly(A)$^+$ RNA was detected by a TAMRA-labeled 2′OMe RNA probe complementary to the poly(A) tail of mRNAs and imaged using a confocal scanning laser microscope. The rationale for using a 2′OMe RNA probe rather than an oligodeoxynucleotide probe is that 2′OMe RNA probes have been reported to possess much higher binding affinities for complementary (RNA) target sequences and to be resistant to nucleases (Majlessi et al., 1998). Furthermore, we have shown previously that microinjection of a TAMRA-labeled 2′OMe $(U)_{22}$ probe in the cytoplasm of U2OS cells results in a nuclear staining pattern characteristic of endogenous poly(A)$^+$ RNA localization (Molenaar et al., 2001).

Previously, oligo (dT) probes have been used to study the movement of poly(A)$^+$ RNA in living cells and, on the basis of these studies, it was concluded that the majority of poly(A)$^+$ RNA is diffusing freely throughout the interchromatin space in cell nuclei (Politz et al., 1998, 1999). However, dependent on the detection method used, different diffusion coefficients for poly(A)$^+$ RNA movement were estimated. Most recently, by using a caged fluorescein-labeled oligo (dT) probe, a diffusion coefficient of 0.6 $\mu m^2/s$ was estimated for poly(A)$^+$ RNA movement (Politz et al., 1999). However, earlier, a diffusion coefficient of 9 $\mu m^2/s$ was measured by fluorescence correlation spectroscopy (Politz et al., 1998). By measuring fluorescence recovery rates in photobleached areas, we report that poly(A)$^+$ RNA is moving through the nucleoplasm at a significantly slower rate of 0.03 $\mu m^2/s$. Therefore, we compared the mobility of 2′OMe RNA probes with that of oligodeoxynucleotide probes under identical conditions. We conclude that the discrepancies in rates of poly(A)$^+$ RNA movement that have been measured in this and previous works can be explained by the differences in hybridization properties in living cells between oligodeoxynucleotide and 2′OMe RNA probes (Molenaar et al., 2001). We suggest that our estimate more accurately reflects the in vivo situation. Our data demonstrate that under conditions of in vivo poly(A)$^+$ RNA imaging, a relatively large fraction of oligo (dT) is highly mobile in the cell nucleus and therefore unbound or transiently bound to poly(A)$^+$ RNA. Importantly, we have shown that the localization and kinetics of the 2′OMe $(U)_{22}$ probe is fully dependent on the presence of a poly(A) tail and that there is at best a very small fraction of unbound probe present that may have led to an overestimation of the poly(A)$^+$ RNA diffusion coefficient. Because hybridization in a living cell is in principle a reversible kinetic process, we cannot exclude that there is some rate of exchange between probe and target molecules during our measurements that can lead to a slight overestimation of the diffusion rate of poly(A)$^+$ RNA.

Recently, it was suggested that the RNA binding proteins PABP2 and TAP move at rates similar to rapidly diffusing poly(A)$^+$ RNA (Calapez et al., 2002). We show that poly(A)$^+$ RNA molecules move at significantly slower rates than previously anticipated, but that PABP2, TAP, and Aly move much more rapidly through the nucleus than poly(A)$^+$ RNA. This finding suggests that a substantial proportion of these proteins is not bound to RNA but is diffusing rapidly throughout the cell nucleus to be available for newly synthesized transcripts.

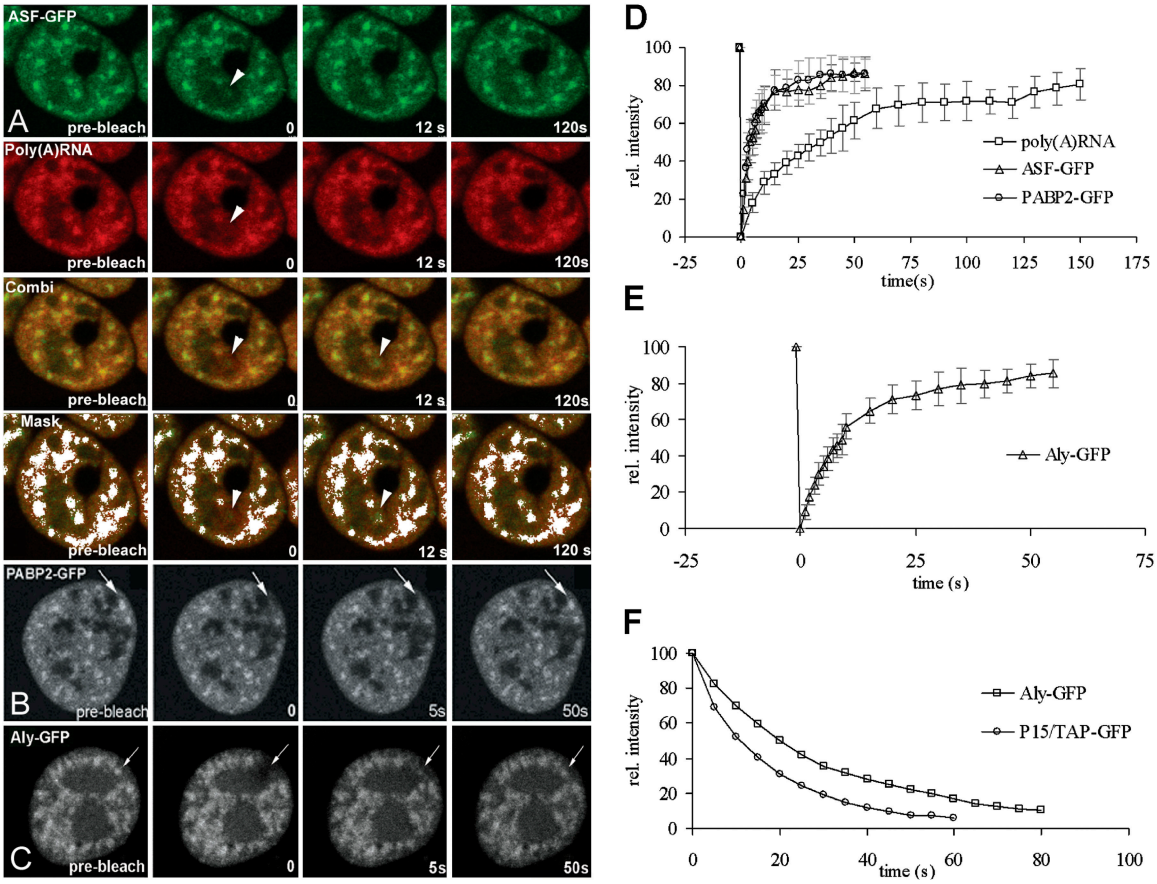

Figure 8. **SF2/ASF, PABP2, and Aly move more rapidly toward speckles than poly(A)$^+$ RNA.** Cells expressing SF2/ASF-GFP were microinjected with 2′OMe $(U)_{22}$-TAMRA and subjected to FRAP analysis (A). SF2/ASF-GFP and 2′OMe $(U)_{22}$-TAMRA were simultaneously bleached in a speckle (arrowheads), and images were recorded before, just after, and at regular time intervals after bleaching. The images taken at 12 s after bleaching indicate that SF2/ASF-GFP (green) has a higher recovery rate compared with poly(A)$^+$ RNA (red). In the combined image at 12 s, the green fluorescence is much stronger than the red. This difference in recovery rate is more evidently shown in the mask images in which areas where both SF2/ASF-GFP and poly(A)$^+$ RNA are present above a threshold value are shown in white. Only after 120 s, a full recovery of fluorescence is observed. (B) FRAP was also performed on cells expressing PABP2-GFP. A speckle was selected (arrow) and photobleached, and the recovery of fluorescence was monitored. As shown, a full recovery of PABP2-GFP fluorescence was obtained within 50 s. Quantitative analysis of recoveries for SF2/ASF-GFP ($n = 8$) or PABP2-GFP ($n = 12$) show similar patterns for both proteins, reaching a plateau at ~90% of the initial fluorescence after ~40 s (D). For reasons of comparison, the recovery plot of poly(A)$^+$ RNA is also shown. Cells expressing Aly-GFP were imaged before and after photobleaching a speckle in the nucleus (C, arrow). The images and the corresponding recovery curve (E) show that fluorescence recovered within 1 min. The error bars in D and E represent SD. The FLIP curve of Aly-GFP shows a complete loss of fluorescence within 80 s, which is a little slower than TAP-GFP (F).

It should be noted that FRAP analysis provides only an average value for poly(A)$^+$ RNA mobility. Some poly(A)$^+$ RNAs may move, within a certain range, faster or slower. Previously, we estimated that abundantly synthesized HCMV IE transcripts move through the nucleus at a diffusion rate of 0.13 $\mu m^2/s$ (Snaar et al., 2002), which is fourfold faster than what we measured for poly(A)$^+$ RNA. In any case, our observations are consistent with studies suggesting that poly(A)$^+$ RNA is not transported by free diffusion but, at least at some stages, by an energy-dependent mechanism (Dargemont and Kühn, 1992; Jarmolowski et al., 1994; Calado et al., 2000; Miralles et al., 2000; Snaar et al., 2002).

Consistent with in situ hybridization studies on fixed cells, we observed that poly(A)$^+$ RNA concentrates in speckles in living cells. Notably, this pattern was not observed when we or others (Politz et al., 1998) used an oligodeoxynucleotide probe instead of a 2′OMe RNA probe for detecting poly(A)$^+$ RNA. Microinjected TAMRA-labeled oligo $(dT)_{40}$ probe revealed a dispersed localization throughout the cell nucleus, but not a staining of speckles. Interestingly, our FRAP and FLIP analyses revealed that the poly(A)$^+$ RNA population inside speckles is mobile and in continuous flux with the nucleoplasm. Only a small amount of the poly(A)$^+$ population that reside in speckles appears to be immobile. Importantly, our observations show that the poly(A)$^+$ population found in speckles is not a stable population of RNAs as suggested previously (Huang et al., 1994). Even when gene transcription is inhibited, poly(A)$^+$ RNA molecules that remain in the nucleus continue to associate and dissociate from speckles and to move throughout the entire nucleus. This observation is consistent with the finding that RNA transport from nucleus to cytoplasm is not dependent on ongoing transcription (Huang and Spector,

1996). Hence, due to their dynamic behavior, it is less likely that the population of poly(A)$^+$ RNA that is localized to speckles plays an essential role in the core organization of speckles by creating binding sites for RNA processing proteins (Sacco-Bubulya and Spector, 2002). In this context, it is worth mentioning that poly(A)$^+$ RNA is not required for the assembly of nuclear speckles in the nuclei of early G1 cells (Ferreira et al., 1994; Gama-Carvalho et al., 1997). Nevertheless, it cannot be excluded that speckle maintenance is a dynamic process and that poly(A)$^+$ RNA plays a role in stabilizing these compartments like mobile heterochromatin protein 1 is responsible for establishing stable heterochromatin domains in cell nuclei (Cheutin et al., 2003; Festenstein et al., 2003).

Another, not necessarily exclusive, possibility is that nuclear poly(A)$^+$ RNA is present in speckles for nonstructural reasons. Because various specific gene transcripts have been found to associate with or to localize to speckles, it has been suggested that speckles play a role in the posttranscriptional processing of RNAs (Xing et al., 1995; Bridge et al., 1996; Smith et al., 1999; Johnson et al., 2000; Hattinger et al., 2002; Shopland et al., 2003). A role for speckles in posttranscriptional splicing is consistent with the observation that splicing factors present in the diffuse nuclear pool of cells lacking speckles are not competent to perform pre-mRNA splicing (Sacco-Bubulya and Spector, 2002). However, there is compelling evidence that the majority of pre-mRNAs are processed cotranscriptionally (Bauren and Wieslander, 1994; Wuarin and Schibler, 1994; Tennyson et al., 1995), and therefore, it is not expected that a high concentration of non- or partially spliced transcripts is present in speckles. Nevertheless, our FRAP and FLIP results show that nearly all nuclear poly(A)$^+$ RNAs move through speckle domains and are therefore consistent with the suggestion that a quality control for correctly spliced or export-competent RNAs takes place in speckles (Johnson et al., 2000). Also, it cannot be excluded that many of the most active, rapidly transcribed genes may have substantial posttransciptional processing. For these purposes, transcripts may transiently interact with some speckle components, and then be released to the nucleoplasm. Interestingly, the import of poly(A)$^+$ RNA into speckles appears to be temperature, and thus energy dependent, which is consistent with the observation that the uptake of microinjected adenovirus pre-mRNAs by speckles was precluded when cells were incubated at 4°C or ATP depleted (Melcak et al., 2001; Kopsky et al., 2002).

In conclusion, speckles may fulfill different functions in the cell nucleus. In addition to playing a role in the assembly, supply, storage, and, possibly, recycling of RNA processing complexes, speckles may represent a checkpoint for whether or not RNAs are appropriately processed and assembled in transport-competent complexes.

The apparently immobile pool of poly(A)$^+$ RNA residing in speckles and nucleoplasm may represent very slow moving RNAs, structural RNAs, as well as incorrectly or slowly processed RNAs. However, the immobile pool may also reflect storage of specific mRNAs. Many mature mRNAs were observed to accumulate in cell nuclei to higher levels than the corresponding precursors (Gondran et al., 1999), and it has been suggested that the nucleus may function as a reservoir for these mRNAs until they are required in the cytoplasm and released by some stimulus. The mechanism by which these mRNAs are retained in the nucleus has not yet been determined though it was shown that some mRNAs are tightly associated with a nuclear matrix structure that remained after nuclear extraction (Gondran et al., 1999). Future work may shed some light on the role that immobile poly(A)$^+$ RNA plays in the cell nucleus.

Materials and methods

Probes

The DNA probe $(dT)_{40}$ and the 2′OMe RNA probes $(U)_{22}$, $(A)_{18}$, U1snRNA (ccugccagguaaguaug), and HCMV-IE (aaacauccucccauca) were synthesized by M. Lemaitre, M. Dechamps, and D. Largana (Eurogentec, Seraing, Belgium). The DNA oligonucleotide $(dT)_{40}$ was synthesized using standard phosphoramidite chemistry and purified by HPLC. 2′OMe RNA probes were synthesized using standard 2′OMe phosphoramidite monomers. TAMRA was covalently linked to the 5′-end of probes via a succinimidyl ester derivative (Molecular Probes). All 2′OMe RNA probes were purified twice by reverse phase HPLC with a Waters 600E instrument. Ion molecular weights of purified probes were determined by mass spectrometry using a Time-Of-Flight instrument (Dynamo).

Construction and expression of GFP fusion proteins

The cDNA encoding SF2/ASF was generated by RT-PCR and cloned into the pEGFP-C1 vector (CLONTECH Laboratories, Inc.) using the EcoRI and BamHI restriction sites as described previously (Molenaar et al., 2001). The cDNA encoding PABP2 was subcloned from a construct provided by E. Wahle (Martin-Luther-Universitat Halle, Halle, Germany) in the pEGFP-C1 vector. The constructs coding for TAP-GFP and p15 were provided by E. Izaurralde (European Molecular Biology Laboratory, Heidelberg, Germany; Braun et al., 2001), and the construct ALY-GFP was a gift from J. Katahira (Osaka University, Osaka, Japan; Zhou et al., 2000). SF2/ASF-GFP was transfected stably into U2OS cells. All other constructs were transiently expressed in U2OS cells using DOTAP (Roche Diagnostics GmbH). Cells were analyzed 24–48 h after transfection and were selected for moderate expression and protein-specific localization.

Cell culture and microinjection

U2OS (human osteosarcoma) cells were cultured on coverslips in 3.5-cm petri dishes (Mattek) in RPMI 1640, without phenol red supplemented with 5% FCS, 0.03% glutamine, and 1000 U/ml penicillin/streptomycin and buffered with 25 mM Hepes buffer to pH 7.2 (all from Life Technologies). Cordycepin (Sigma-Aldrich) was used at 50 μg/ml. Microinjection of probes was performed as described previously (Molenaar et al., 2001). Cells showing moderate levels of fluorescence were selected and analyzed by digital fluorescence microscopy on the day of microinjection.

Live cell imaging

Cells were monitored using a confocal microscope system (model TCS/SP2; Leica). Cells were scanned in 2D in time, with a pinhole setting of 2.5 Airy. During the experiment, the temperature of the cells was maintained at 37°C using a heated ring surrounding the culture chamber (Harvard App. Inc.) and a microscope objective heater (Bioptechs) unless indicated otherwise. The 543-nm He Ne laser was used for TAMRA excitation with the emission window set between 560–630 nm. GFP was scanned with the 488-nm line of an Argon laser with the emission window set between 500–540 nm. In the double-labeling experiment, GFP and TAMRA were sequentially scanned to avoid cross talk. Images were acquired using a 100× NA 1.4PL APO lens and analyzed with Leica software. Images were further analyzed using Leica software and Adobe Photoshop. To show colocalization, masked images were obtained using the Leica multi-color software package.

Photobleaching experiments and quantitative analysis

For spot bleaching in FRAP and FLIP analysis, the laser beam parking option on the confocal microscope was used. The 543- and the 488-nm lasers were set at 100%, and the duration of the spot bleaching was set such that bleaching resulted in a nearly complete loss of fluorescence in the defined area. In practice, TAMRA-labeled probes were bleached for 5 s and GFP fusion proteins for 3 s. Subsequent images where recorded before, just after, and at different time intervals after bleaching. The length of the time

intervals was established depending on the speed of recovery of the fluorescence. For example, for imaging poly(A)$^+$ RNA, 24 images were acquired in three series with increasing time intervals (10 images every 2 s, 10 images every 10 s, and then 4 images every 30 s). For imaging GFPs and control probes, the time intervals were shorter (indicated in the FRAP curves in Results). Quantitative analysis of fluorescence intensities was performed using Leica software and Excel. FRAP recovery intensities were corrected for background intensities. The total cellular fluorescence was measured before and immediately after the bleach pulse to correct for loss of fluorescence during the bleach pulse and during imaging. For determination of the $t_{1/2}$ values and for the immobile fractions, the intensity values before bleaching were set at 100% and the intensity values directly after bleaching were set at 0%. All intensities measured during recovery were transformed to relative intensities. The $t_{1/2}$ values, indicating the time points at which 50% of the end-fluorescence intensity (*Fend*) was reached, were determined from the FRAP curves. Estimation of the effective diffusion coefficients (D_{eff}) from FRAP experiments was performed as described by Yguerabide et al. (1982) using the formula $D = \beta w^2/4t_{1/2}$, where w is the radius of the bleached area at e^{-2} intensity and β is a parameter that depends on the percent bleach. The values for β were determined for each experiment from a theoretical plot generated from data presented by Yguerabide et al. (1982), and w was estimated using fixed cells expressing GFP. For FLIP experiments, cells were repeatedly imaged and bleached at intervals of 2 s for measuring loss of GFP signal and of 3 s for measuring loss of TAMRA fluorescence. For curve fitting, the program CurveExpert 1.3 has been used.

We are grateful to E. Izaurralde for providing TAP-GFP and p15, to J. Katahira for providing Aly-GFP, and to S. van Koningsbruggen for generating the PABP2-GFP construct. We thank K. Wiesmeijer for excellent technical assistance and M. Lemaitre, M. Dechamps, and D. Largana for the synthesis of the probes used in this work. We are also thankful to David Baker for critical reading of the manuscript.

This work was supported by the Netherlands Organization of Scientific Research program 4D Imaging of Living Cells and Tissues (grant 901-34-144).

Submitted: 29 October 2003
Accepted: 22 March 2004

References

Bauren, G., and L. Wieslander. 1994. Splicing of Balbiani ring 1 gene pre-mRNA occurs simultaneously with transcription. *Cell.* 76:183–192.

Bauren, G., W.Q. Jiang, K. Bernholm, F. Gu, and L. Wieslander. 1996. Demonstration of a dynamic, transcription-dependent organization of pre-mRNA splicing factors in polytene nuclei. *J. Cell Biol.* 133:929–941.

Braun, I.C., A. Herold, M. Rode, E. Conti, and E. Izaurralde. 2001. Overexpression of TAP/p15 heterodimers bypasses nuclear retention and stimulates nuclear mRNA export. *J. Biol. Chem.* 276:20536–20543.

Bridge, E., K.U. Riedel, B.M. Johansson, and U. Petterson. 1996. Spliced exons of adenovirus late RNAs colocalize with snRNP in a specific nuclear domain. *J. Cell Biol.* 135:303–314.

Calado, C., and M. Carmo-Fonseca. 2000. Localization of poly(A)-binding protein 2 (PABP2) in nuclear speckles is independent of import into the nucleus and requires binding to poly(A) RNA. *J. Cell Sci.* 113:2309–2318.

Calado, A., U. Kutay, U. Kuhn, E. Wahle, and M. Carmo-Fonseca. 2000. Deciphering the cellular pathway for transport of poly(A)-binding protein II. *RNA.* 6:245–256.

Calapez, A., H.M. Pereira, A. Calado, J. Braga, J. Rino, C. Carvalho, J.P. Tavanez, E. Wahle, A.C. Rosa, and M. Carmo-Fonseca. 2002. The intranuclear mobility of messenger RNA binding proteins is ATP dependent and temperature sensitive. *J. Cell Biol.* 159:795–805.

Carter, K.C., K.L. Taneja, and J.B. Lawrence. 1991. Discrete nuclear domains of poly(A) RNA and their relationship to the functional organization of the nucleus. *J. Cell Biol.* 115:1191–1202.

Carter, K.C., D. Bowman, W. Carrington, K. Fogarty, J.A. McNeil, F.S. Fay, and J.B. Lawrence. 1993. A three-dimensional view of precursor messenger RNA metabolism within the mammalian nucleus. *Science.* 259:1330–1335.

Cmarko, D., P.J. Verschure, T.E. Martin, M.E. Dahmus, S. Krause, X.D. Fu, R. van Driel, and S. Fakan. 1999. Ultrastructural analysis of transcription and splicing in the cell nucleus after bromo-UTP microinjection. *Mol. Biol. Cell.* 10:211–223.

Cheutin, T., A.J. McNair, T. Jenuwein, D.M. Gilbert, P.B. Singh, and T. Misteli. 2003. Maintenance of stable heterochromatin domains by dynamic HP1 binding. *Science.* 299:721–725.

Cullen, B.R. 2003. Nuclear RNA export. *J. Cell Sci.* 116:587–597.

Custodio, N., M. Carmo-Fonseca, F. Geraghty, H.S. Pereira, F. Grosveld, and M. Antoniou. 1999. Inefficient processing impairs release of RNA from the site of transcription. *EMBO J.* 18:2855–2866.

Dargemont, C., and L.C. Kühn. 1992. Export of mRNA from microinjected nuclei of *Xenopus laevis* oocytes. *J. Cell Biol.* 118:1–9.

Darnell, J.E., L. Philipson, R. Wall, and M. Adesnik. 1971. Polyadenylic acid sequences: role in conversion of nuclear RNA into messenger RNA. *Science.* 174:507–510.

Dirks, R.W., K.C. Daniel, and A.K. Raap. 1995. RNAs radiate from gene to cytoplasm as revealed by fluorescence in situ hybridization. *J. Cell Sci.* 108: 2565–2572.

Dirks, R.W., E.S. de Pauw, and A.K. Raap. 1997. Splicing factors associate with nuclear HCMV-IE transcripts after transcriptional activation of the gene, but dissociate upon transcription inhibition: evidence for a dynamic organization of splicing factors. *J. Cell Sci.* 110:515–522.

Fakan, S. 1994. Perichromatin fibrils are in situ forms of nascent transcripts. *Trends Cell Biol.* 4:86–90.

Ferreira, J.A., M. Carmo-Fonseca, and A.I. Lamond. 1994. Differential interaction of splicing snRNPs with coiled bodies and interchromatin granules during mitosis and assembly of daughter cell nuclei. *J. Cell Biol.* 126:11–23.

Festenstein, R., S.N. Pagakis, K. Hiragami, D. Lyon, A. Verreault, B. Sekkali, and D. Kioussis. 2003. Modulation of heterochromatin protein 1 dynamics in primary mammalian cells. *Science.* 299:719–721.

Gama-Carvalho, M., R.D. Krauss, L. Chiang, J. Valcarcel, M.R. Green, and M. Carmo-Fonseca. 1997. Targeting of U2AF^{65} to sites of active splicing in the nucleus. *J. Cell Biol.* 137:975–987.

Gatfield, D., and E. Izaurralde. 2002. REF1/Aly and the additional exon junction complex proteins are dispensable for nuclear mRNA export. *J. Cell Biol.* 159: 579–588.

Gondran, P., F. Amiot, D. Weil, and F. Dautry. 1999. Accumulation of mature mRNA in the nuclear fraction of mammalian cells. *FEBS Lett.* 458:324–328.

Hattinger, C.M., A.G. Jochemsen, H.J. Tanke, and R.W. Dirks. 2002. Induction of p21 mRNA synthesis after short-wavelength UV light visualized in individual cells by RNA FISH. *J. Histochem. Cytochem.* 50:81–89.

Huang, S., and D.L. Spector. 1996. Intron-dependent recruitment of pre-mRNA splicing factors to sites of transcription. *J. Cell Biol.* 131:719–732.

Huang, S., T.J. Deerinck, M.H. Ellisman, and D.L. Spector. 1994. In vivo analysis of the stability and transport of nuclear poly(A)$^+$ RNA. *J. Cell Biol.* 126: 877–899.

Huang, Y., R. Gattoni, J. Stevenin, and J.A. Steitz. 2003. SR splicing factors serve as adapter proteins for TAP-dependent mRNA export. *Mol. Cell.* 11:837–843.

Jarmolowski, A., W.C. Boelens, E. Izaurralde, and I.W. Mattaj. 1994. Nuclear export of different classes of RNA is mediated by specific factors. *J. Cell Biol.* 124:627–635.

Jimenez-Garcia, L.F., and D.L. Spector. 1993. In vivo evidence that transcripts and splicing are coordinated by a recruiting mechanism. *Cell.* 73:47–59.

Johnson, C., D. Primorac, M. McKinstry, J. McNeil, D. Rowe, and J.B. Lawrence. 2000. Tracking COL1A1 RNA in osteogenesis imperfecta: splice-defective transcripts initiate transport from the gene but are retained within the SC35 domain. *J. Cell Biol.* 150:417–432.

Katahira, J., K. Stasser, A. Podtelejnikov, M. Mann, J.U. Jung, and E. Hurt. 1999. The Mex67p-mediated nuclear export pathway is conserved from yeast to human. *EMBO J.* 18:2593–2609.

Kopsky, V., J. Vecerova, I. Melcak, A. Pliss, J. Stulik, K. Koberna, L. Tomaskova, and I. Raska. 2002. An ATP-dependent step is required for the translocation of microinjected precursor mRNA into nuclear speckles. *Folia Biol. (Praha).* 48:69–72.

Lamond, A.I., and M. Carmo-Fonseca. 1993. Localisation of splicing snRNPs in mammalian cells. *Mol. Biol. Rep.* 18:127–133.

Lamond, A.I., and D.L. Spector. 2003. Nuclear speckles: a model for nuclear organelles. *Nat. Rev. Mol. Cell Biol.* 4:605–612.

Le Hir, H., D. Gatfield, I.C. Braun, D. Forler, and E. Izaurralde. 2001. The protein Mago provides a link between splicing and mRNA localization. *EMBO Rep.* 2:1119–1124.

Lei, E.P., and P.A. Silver. 2002. Intron status and 3′-end formation control cotranscriptional export of mRNA. *Genes Dev.* 16:2761–2766.

Lei, E.P., H. Krebber, and P.A. Silver. 2001. Messenger RNAs are recruited for nuclear export during transcription. *Genes Dev.* 15:1771–1782.

Luo, M.L., and R. Reed. 1999. Splicing is required for rapid and efficient mRNA export in metazoans. *Proc. Natl. Acad. Sci. USA.* 96:14937–14942.

Luo, M.L., Z. Zhou, K. Magni, C. Christoforides, J. Rappsilber, M. Mann, and R. Reed. 2001. Pre-mRNA splicing and mRNA export linked by direct interactions between UAP56 and Aly. *Nature.* 413:644–647.

Macville, M.V.E., K.C. Wiesmeijer, J.A.M. Fransen, R.W. Dirks, and A.K. Raap. 1995. Detection of specific mRNA by electron microscopic in situ hybridization: implications for nucleocytoplasmic transport. *Eur. J. Cell Biol.* 68: 470–474.

Majlessi, M., N.C. Nelson, and M.M. Becker. 1998. Advantages of 2'-O-methyl oligoribonucleotide probes for detecting RNA targets. *Nucleic Acids Res.* 26: 2224–2229.

Melcak, I., S. Cermanova, K. Jirsova, K. Koberna, J. Malinsky, and I. Raska. 2000. Nuclear pre-mRNA compartmentalization: trafficking of released transcripts to splicing factor reservoirs. *Mol. Biol. Cell.* 11:497–510.

Melcak, I., S. Melcakova, V. Kopsky, J. Vecerova, and I. Raska. 2001. Prespliceosomal assembly on microinjected precursor mRNA takes place in nuclear speckles. *Mol. Biol. Cell.* 12:393–406.

Mendecki, J., S.Y. Lee, and G. Brawerman. 1972. Characteristics of the polyadenylic acid segment associated with messenger ribonucleic acid in mouse sarcoma 180 ascites cells. *Biochemistry.* 11:792–798.

Miralles, F., L.G. Ofverstedt, N. Sabri, Y. Aissouni, U. Hellman, U. Skoglund, and N. Visa. 2000. Electron tomography reveals posttranscriptional binding of pre-mRNPs to specific fibers in the nucleoplasm. *J. Cell Biol.* 148:271–282.

Misteli, T., J.F. Caceres, and D.L. Spector. 1997. The dynamics of a pre-mRNA splicing factor in living cells. *Nature.* 387:523–527.

Molenaar, C., S.A. Marras, J.C. Slats, J.C. Truffert, M. Lemaitre, A.K. Raap, R.W. Dirks, and H.J. Tanke. 2001. Linear 2' O-Methyl RNA probes for the visualization of RNA in living cells. *Nucleic Acids Res.* 29:E89.

Ohno, M., A. Segref, S. Kuersten, and I.W. Mattaj. 2002. Identity elements used in export of RNAs. *Mol. Cell.* 9:659–671.

Politz, J.C., E.S. Browne, D.E. Wolf, and T. Pederson. 1998. Intranuclear diffusion and hybridization state of oligonucleotides measured by fluorescence correlation spectroscopy in living cells. *Proc. Natl. Acad. Sci. USA.* 95:6043–6048.

Politz, J.C., R.A. Tuft, T. Pederson, and R.H. Singer. 1999. Movement of nuclear poly(A) RNA throughout the interchromatin space in living cells. *Curr. Biol.* 9:285–291.

Puvion, E., and F. Puvion-Dutilleul. 1996. Ultrastructure of the nucleus in relation to transcription and splicing: roles of perichromatin fibrils and interchromatin granules. *Exp. Cell Res.* 229:217–225.

Sacco-Bubulya, P., and D.L. Spector. 2002. Disassembly of interchromatin granule clusters alters the coordination of transcription and pre-mRNA splicing. *J. Cell Biol.* 156:425–436.

Sehgal, P.B., J.E. Darnell, and I. Tamm. 1976. The inhibition by DRB (5,6-dichloro-1-beta-D-ribofuranosylbenzimidazole) of hnRNA and mRNA production in HeLa cells. *Cell.* 9:473–480.

Shopland, L.S., C.V. Johnson, and J.B. Lawrence. 2002. Evidence that all SC-35 domains contain mRNAs and that transcripts can be structurally constrained within these domains. *J. Struct. Biol.* 140:131–139.

Shopland, L.S., C.V. Johnson, M. Byron, J. McNeil, and J.B. Lawrence. 2003. Clustering of multiple specific genes and gene-rich R-bands aroend SC-35 domains: evidence for local euchromatic neighborhoods. *J. Cell Biol.* 162: 981–990.

Singh, O.P., B. Bjorkroth, S. Masich, L. Wieslander, and B. Daneholt. 1999. The intranuclear movement of Balbiani ring premessenger ribonucleoprotein particles. *Exp. Cell Res.* 251:135–146.

Smith, K.P., P.T. Moen, K.L. Wydner, J.R. Coleman, and J.B. Lawrence. 1999. Processing of endogenous pre-mRNAs in association with SC-35 domains is gene specific. *J. Cell Biol.* 144:617–629.

Snaar, S.P., M. Vincent, and R.W. Dirks. 1999. RNA polymerase II localizes at sites of human cytomegalovirus immediate-early RNA synthesis and processing. *J. Histochem. Cytochem.* 47:245–254.

Snaar, S.P., P. Verdijk, H.J. Tanke, and R.W. Dirks. 2002. Kinetics of HCMV immediate early mRNA expression in stably transfected fibroblasts. *J. Cell Sci.* 115:321–328.

Strasser, K., S. Masuda, P. Mason, J. Phannstiel, M. Oppizzi, S. Rodriguez-Navarro, A.G. Rondon, A. Aguilera, K. Struhl, R. Reed, and E. Hurt. 2002. TREX is a conserved complex coupling transcription with messenger RNA export. *Nature.* 417:304–308.

Tennyson, C.N., H.J. Klamut, and R.G. Worton. 1995. The human dystrophin gene requires 16 hours to transcribe and is cotranscriptionally spliced. *Nat. Genet.* 9:184–190.

Wei, X., S. Somanathan, J. Samarabandu, and R. Berezney. 1999. Three-dimensional visualization of transcription sites and their association with splicing factor–rich nuclear speckles. *J. Cell Biol.* 146:543–558.

Wuarin, J., and U. Schibler. 1994. Physical isolation of nascent RNA chains transcribed by RNA polymerase II: evidence for cotranscriptional splicing. *Mol. Cell. Biol.* 14:7219–7225.

Xing, Y., C.V. Johnson, P.R. Dobner, and J.B. Lawrence. 1993. Higher level organization of individual gene transcription and RNA splicing. *Science.* 259: 1326–1330.

Xing, Y., C.V. Johnson, P.T. Moen, J.A. McNeil, and J.B. Lawrence. 1995. Nonrandom gene organization: structural arrangements of specific pre-mRNA transcription and splicing with SC-35 domains. *J. Cell Biol.* 131:1635–1647.

Yguerabide, J., J.A. Schmidt, and E.E. Yguerabide. 1982. Lateral mobility in membranes as detected by fluorescence recovery after photobleaching. *Biophys. J.* 40:69–75.

Zachar, Z., J. Kramer, I.P. Mims, and P.M. Bingham. 1993. Evidence for channeled diffusion of pre-mRNAs during nuclear RNA transport in metazoans. *J. Cell Biol.* 121:729–742.

Zeng, C., E. Kim, S.L. Warren, and S.M. Berget. 1997. Dynamic relocation of transcription and splicing factors dependent upon transcriptional activity. *EMBO J.* 16:1401–1412.

Zhou, Z., M.J. Luo, K. Straesser, J. Katahira, E. Hurt, and R. Reed. 2000. The protein Aly links pre-messenger-RNA splicing to nuclear export in metazoans. *Nature.* 407:401–405.